1-1-1977

Effects and applications of geometry variations on the combined forward-backward extrusion.

Carlos Enrique Umana

EFFECTS AND APPLICATIONS OF GEOMETRY VARIATIONS ON THE COMBINED FORWARD-BACKWARD EXTRUSION

by
Carlos Enrique Umana

A Thesis
Presented to the Graduate Committee
of Lehigh University
in Candidacy for the Degree of
Master of Science
in
Metallurgy and Materials Science

Lehigh University
1977

CERTIFICATE OF APPROVAL

This thesis is accepted and approved in partial fulfillment of the requirements for the degree of Master of Science.

APRIL 15, 1977
(date)

Professor in Charge

Chairman of Department

ACKNOWLEDGEMENTS

The author wishes to express his gratitude to his advisor, Professor Betzalel Avitzur, for his continued encouragement and guidance throughout the course of this study. The author is also indebted to The Latin American Scholarship Program of American Universities (LASPAU) for the scholarship of which he was recipient and to the University of Costa Rica for partial financial support during this study.

Use of the UBET computer program was made possible by AISI.

The author expresses thanks to his parents for their encouragement.

Finally, the author expresses his deepest thanks to his wife, Gilda, for her extreme patience, help, and understanding throughout the past two years.

TABLE OF CONTENTS

LIST OF TABLES

LIST OF FIGURES

NOMENCLATURE

H_1 = height of lower die wall (see Fig. 2)

H_2 = height of upper die wall (see Fig. 2)

h_1 = see Fig. 2

h_2 = height of the ram (see Fig. 2)

L = tube length (see Fig. 5)

m = friction factor

p_R = average ram pressure

R_i = mandrel radius

R_o = upper die radius

R_1 = lower die radius

R_2 = ram radius

$(R_o/R_2)_{crit.}$ = relative critical upper radius for flash formation

$(R_o/R_2)_{cbe}$ = relative critical upper radius for backward extrusion

T = distance between ram and lower die

T_o = initial slug thickness

$\dot{U}$ = ram velocity

v_b = backward velocity

v_f = forward velocity

VSUBT = relative velocity at the top surface

VSUBL = relative velocity at the left surface

VSUBB = relative velocity at the bottom surface

VSUBR = relative velocity at the right surface

WF = friction pressure component

WI = internal deformation pressure component

WS = shear pressure component

x = variable dimension (see Fig. 10)

ΔT = displacement of the ram with respect to T_o

Γ_i = boundaries of velocity discontinuity

σ_o = yield strength in uniaxial tension

ABSTRACT

A numerical study of combined forward-backward extrusion based on the reviewed analytical solution originally provided by Avitzur, Hahn, and Mori and on the 'Upper Bound Elemental Technique' (UBET) computer program is described in this paper. Emphasis is given to the changing nature of the extrusion as a process rather than to consideration of single instantaneous stages only. Results of a computer simulation of the tube extrusion process based on the former analytical solution and including the effect of the active friction between the tube and mandrel are presented. It has been found that the active friction can have a pronounced effect in the early stages of the extrusion. The concept of critical upper gap for forward extrusion with and without backward flash and for forward-backward extrusion is introduced. For a given slug thickness, the lower the friction, the larger is the critical upper gap for forward extrusion without flash.

The effect of tapered tool surfaces on extrusion force and metal flow is demonstrated using the UBET approach. Suggestions for optimization of the energy or force of a complete process are given.

INTRODUCTION

The Process

A combined forward-backward extrusion, as the name implies, involves a combination of forward and reverse metal flow (see Fig. 1). The slug, which is to be extruded, is placed in a die and a moving ram forces the metal to flow through the die openings around the ram and punch under a compressive pressure. This method is used to produce complex-shape extrudates. If the raw material is a solid slug then a cup and rod assembly is formed as a single piece. If a hollow slug is the raw material then a tubular part is obtained. The wall thickness of the extrudates is determined by the clearance between the ram, punch and die. The upper and lower clearance dimensions not only determine the final geometry of the product but also determine the relative amounts of metal displaced forward and backward.

The design of the die and the ram is determined primarily by the final shape of the part to be extruded. However, when an intermediate process is considered or the product design allows for certain die and ram variations, it is convenient to go from square-cornered dies and rams to tapered shapes. As Fig. 1 shows, it is evident that tapered die or ram faces with the right design can assure an optimal plastic metal flow that minimizes the extrusion pressure with respect to a flat die and therefore reduces the manufacturing cost and/or increases the reduction and size of the part. Furthermore, the tool shape will

determine the relative amounts of forward and backward metal flow. As a result the relative metal flow in Fig. 1a could be different from that in Fig. 1b, even though the radial dimensions are the same.

The process of forward extrusion of rod or tube is obtained when the ram fits the wall of the die in such a way that no metal flows backward. This design is used for forming compact or hollow parts with or without a flange. On a large scale (Ref. 1), the process is used to produce seamless pipe for special applications. Pipes of more than one meter internal diameter and more than twenty meters long are made by this method.

On the other hand, if the mandrel fits the lower die wall all the metal flows backward as in the backward impact extrusion process.

The Upper-Bound Analytical Solution

The upper-bound analysis has been used to predict the maximum power required during a metal-forming process. The actual power required can be equal to or lower than that predicted by the upper-bound solution, which is given by the sum of the shear, friction, and internal deformation power components. According to the upper-bound theorem, metal flow will take the pattern which minimizes the relative ram pressure for a given geometry and friction. Upper-bound solutions are functions of the independent and pseudoindependent parameters. Geometry factors, friction, and flow strength of the material are the independent process parameters. The relative speed of the

emerging material, upwards or downwards, is the pseudoindependent process parameter. The actual value of a given solution is obtained by a process of minimization on the total power with respect to the pseudoindependent parameter. The upper-bound analysis for the combined forward-backward extrusion was provided by Avitzur, B., W.C. Hahn, Jr., and Masahiro Mori (Ref. 2). The solution predicts the required relative ram pressure as a function of the process geometry. Figure 2 illustrates the process and shows the deforming body divided into regions which are separated by surfaces of velocity discontinuity (Ref. 3). Metal in zones II, III, IV is undergoing deformation; metal in zones I and V has already completed its deformation.

The complete analysis of the velocity field, internal deformation, friction losses, and shear losses is presented in Ref. 2. The expression for the total average relative pressure provided through the ram according to Ref. 2 was reviewed in this study.

The resulting relationship is given by Equation 1 as follows:

$$\frac{p_R}{\sigma_o} = \frac{1}{\sqrt{3}\left(1 - \left(\frac{R_i}{R_2}\right)^2\right)} \left\{ \left(\frac{R_i}{R_2}\right)^2 \left| \frac{1 - \left(\frac{R_1}{R_2}\right)^2 - \left[1 - \left(\frac{R_o}{R_2}\right)^2\right] \frac{v_b}{\dot{U}}}{\left(\frac{R_1}{R_2}\right)^2 - \left(\frac{R_i}{R_2}\right)^2} \right| \right.$$

$$\cdot \left| (2 - \sqrt{1 + 3\left(\frac{R_1}{R_2}\right)^4 \left(\frac{R_2}{R_i}\right)^4} + \ell n \left| \frac{1}{3} \left(\frac{R_i}{R_2}\right)^2 \left(\frac{R_2}{R_1}\right)^2 \right.\right.$$

$$\left.\left. \cdot \left(1 + \sqrt{1 + 3\left(\frac{R_1}{R_2}\right)^4 \left(\frac{R_2}{R_i}\right)^4}\right) \right| \right) \left| + \left| (1 - [1 - \left(\frac{R_o}{R_2}\right)^2] \frac{v_b}{\dot{U}}) \right| \right.$$

$$\cdot \left[\sqrt{1 + 3 \left(\frac{\left(\frac{R_1}{R_2}\right)^2}{1 - [1 - \left(\frac{R_o}{R_2}\right)^2] \frac{v_b}{\dot{U}}} \right)^2} \right.$$

$$\left. - \sqrt{1 + \frac{3}{\left(1 - [1 - \left(\frac{R_o}{R_2}\right)^2] \frac{v_b}{\dot{U}}\right)^2}} + \ell n \left| \left(\frac{R_1}{R_2}\right)^2 \right| \right.$$

$$\cdot \frac{1 + \sqrt{1 + \dfrac{3}{\left(1 - \left[1 - \left(\dfrac{R_o}{R_2}\right)^2\right] \dfrac{v_b}{\dot{U}}\right)^2}}}{1 + \sqrt{1 + 3\left(\dfrac{\left(\dfrac{R_1}{R_2}\right)^2}{1 - \left[1 - \left(\dfrac{R_o}{R_2}\right)^2\right] \dfrac{v_b}{\dot{U}}}\right)^2}} \left| \left[\right] \right| + \left| \frac{v_b}{\dot{U}} \left(\frac{R_o}{R_2}\right)^2 \right|$$

$$\cdot \left(2 - \sqrt{1 + 3\left(\frac{R_2}{R_o}\right)^4} - \ell n \left| \left(\frac{R_2}{R_o}\right)^2 \frac{3}{1 + \sqrt{1 + 3\left(\frac{R_2}{R_o}\right)^4}} \right| \right) \Bigg|$$

$$+ m \left[\left| \frac{1 - \left(\dfrac{R_i}{R_2}\right)^2 - \left[1 - \left(\dfrac{R_o}{R_2}\right)^2\right] \dfrac{v_b}{\dot{U}}}{\left(\dfrac{R_1}{R_2}\right)^2 - \left(\dfrac{R_i}{R_2}\right)^2} \right| \cdot 2 \frac{R_1}{R_2} \frac{H_1}{R_2} + \right.$$

$$\left(2 \frac{R_i}{R_2} \frac{h_1}{R_2} + \frac{R_i}{R_2} \frac{T}{R_2} + \frac{R_2}{3T} \left(2 \frac{R_i}{R_2} + \frac{R_1}{R_2}\right) \left(\frac{R_1}{R_2} - \frac{R_i}{R_2}\right)^2 \right) \cdot \left| \frac{1 - \left(\dfrac{R_1}{R_2}\right)^2 - \left[1 - \left(\dfrac{R_o}{R_2}\right)^2\right] \dfrac{v_b}{\dot{U}}}{(R_1/R_2)^2 - (R_i/R_2)^2} \right|$$

$$+ \frac{2}{3} \frac{R_2}{T} \left| \left(1 - \frac{R_1}{R_2}\right) \left(2 - \frac{R_1}{R_2} - \left(\frac{R_1}{R_2}\right)^2 - 3 \left[1 - \left(\frac{R_o}{R_2}\right)^2\right] \frac{v_b}{\dot{U}}\right) \right| + \left| \frac{R_2}{3T} \frac{v_b}{\dot{U}} \right.$$

$$\cdot \left[1 - 3\left(\frac{R_o}{R_2}\right)^2 + 2\left(\frac{R_o}{R_2}\right)^3\right] \Bigg| + \frac{R_o}{R_2}\frac{T}{R_2}\left|\frac{v_b}{\dot{U}}\right| + 2\frac{h_2}{R_2}\left|1 - \frac{v_b}{\dot{U}}\right|$$

$$+ 2\left|\frac{v_b}{\dot{U}}\right| \times \frac{R_o}{R_2}\left|\frac{H_2}{R_2} - \frac{T}{R_2}\right| \Bigg] + \left|1 - \left(\frac{R_1}{R_2}\right)^2 - \left[1 - \left(\frac{R_o}{R_2}\right)^2\right]\frac{v_b}{\dot{U}}\right|$$

$$\cdot \left| \frac{1}{3}\frac{R_2}{T}\left(2\frac{R_i}{R_2} + \frac{R_1}{R_2}\right)\frac{\frac{R_i}{R_2} - \frac{R_1}{R_2}}{\frac{R_i}{R_2} + \frac{R_1}{R_2}}\right| + \left|\frac{R_1}{R_2}\frac{T}{R_2} \cdot \frac{1-\left(\frac{R_i}{R_2}\right)^2 - \left[1-\left(\frac{R_o}{R_2}\right)^2\right]\frac{v_b}{\dot{U}}}{\left(\frac{R_1}{R_2}\right)^2 - \left(\frac{R_i}{R_2}\right)^2}\right|$$

$$+ \left| 1 - \frac{v_b}{\dot{U}}\right| \left|\frac{T}{R_2} + \frac{1}{3}\right| \left|\frac{v_b}{\dot{U}}\right| \left|\frac{R_2}{T}\right| \left| 1 - 3\left(\frac{R_o}{R_2}\right)^2 + 2\left(\frac{R_o}{R_2}\right)^3\right| \Bigg\} \qquad (1)$$

In symbolic form, Eq. (1) reads as follows:

$$\frac{p_R}{\sigma_o} = f\left(\frac{R_i}{R_2}, \frac{R_1}{R_2}, \frac{R_o}{R_2}, \frac{H_1}{R_2}, \frac{H_2}{R_2}, \frac{h_1}{R_2}, \frac{h_2}{R_2}, \frac{T}{R_2}, m, \frac{v_b}{\dot{U}}\right)$$

Upper Bound Elemental Technique (UBET)

Equation (1) applies only for flat dies and rams. When tapered or more complex parts are considered, the solution could be obtained by using the UBET computer program (Ref. 4). This program handles rectangular as well as triangular elements of axisymmetric configurations including the combined forward-backward extrusion.

The purpose of this paper is to realize a numerical study of combined forward-backward extrusion and the tube-flange forming process by using the analytical solution of Ref. 2 and the UBET computer program (Ref. 4). The tubular forming process is considered as a special case of the combined forward-backward extrusion process.

For detailed coverage of the use of the upper-bound approach to metal-forming processes and its developments see Refs. 3, 5, and 6.

RESULTS

In Ref. 2 the value of $v_b/\dot{U}$ which optimizes the relative extrusion pressure (p_R/σ_o) was found from plots of (p_R/σ_o) as a function of $v_b/\dot{U}$. A similar plot is shown in Fig. 3 of this paper. Presently an intercom computer program based on Eq. (1) was developed to determine the optimal $v_b/\dot{U}$ as a function of the other process parameters and to evaluate the behavior of the main variables associated with the tube-extrusion process, which was studied as a special case of combined forward-backward extrusion with or without flash formation. A flow chart of the computer program is shown in the Appendix.

Variations in the front and back exit speed vs. wall thickness of the top emerging tube are described by Fig. 4.

In order to study the tubular extrusion process by using the general combined forward-backward extrusion solution, it was necessary to choose the gap between the ram and the chamber small enough to prevent backward extrusion and flash. According to Fig. 2 this gap can be expressed as

$$\text{Gap} = R_o/R_2 - 1 \tag{2}$$

Ideally, a tube forming process is accomplished when

$$1 < R_o/R_2 \leq (R_o/R_2)_{crit.}$$

where $(R_o/R_2)_{crit.}$ represents the maximum R_o/R_2 value for which

$(v_b/\dot{U})_{opt.} = 1.$

As in practice, the description of the tube-extrusion process must start by considering a hollow disk slug of thickness T_o/R_2. As it is deduced from Fig. 5, the portion of the ram of R_i/R_2 radius, which is known as the mandrel, was taken equal to or greater than T_o/R_2 in this study. If the condition $R_o/R_2 \leq (R_o/R_2)_{crit.}$ is satisfied, then once the extrusion begins all the material will move down at the velocity $v_f/\dot{U}$, which according to volume constancy is given by

$$v_f/\dot{U} = \frac{1 - (R_i/R_2)^2 - v_b/\dot{U}\,[1 - (R_o/R_2)^2]}{(R_1/R_2)^2 - (R_i/R_2)^2} \tag{3}$$

The instantaneous length of the tube L/R_2 (Fig. 5) can be obtained as a function of the instantaneous thickness of the billet T/R_2 by using the volume constancy principle as presented by the following equation:

$$L/R_2 = (T/R_2)\,\frac{(R_o/R_2)^2 - (R_i/R_2)^2}{(R_1/R_2)^2 - (R_i/R_2)^2} \tag{4}$$

Assuming that R_o/R_2 is constant in any process, no matter what the value of T/R_2, it was necessary to analyze how the critical gap is affected as the slug thickness decreases. The variation of $(R_o/R_2)_{crit.}$ for a given geometry is presented in Fig. 6 with friction as a para-

meter.

It is important to observe in Fig. 5 that while H_1/R_2 is constant, T/R_2, L/R_2, and h_1/R_2 are changing during the process and that h_1/R_2 increases continuously in the same amount that T/R_2 decreases. All this, combined with the fact that h_1/R_2, initially, can be greater or smaller than H_1/R_2, leads to various possibilities when the dimensions h_1/R_2, H_1/R_2 and L/R_2 are considered together in describing the process. These possible situations are summarized in Table 1 and were applied in the computer simulation program of the tube extrusion process made in this study. As it will be observed later, all these factors can introduce pronounced effect on the extrusion pressure for large friction values.

Since in the tubular process it is supposed that no metal is coming up (backward), the value of h_2/R_2 was taken as zero and that of H_2/R_2 as equal to T/R_2 in Eq. (1) in order to simplify the analysis. In other words, these parameters do not affect the extrusion pressure if $R_o/R_2 \leq (R_o/R_2)_{crit.}$.

In addition to $(R_o/R_2)_{crit.}$ another parameter called $(R_o/R_2)_{cbe}$ (critical radius for backward extrusion) was computed. This parameter is defined as the maximum radius R_o/R_2 for which $v_b/\dot{U} = 0$ (see Fig. 4). The parameter is plotted in Fig. 7 together with $(R_o/R_2)_{crit.}$ as a function of the slug thickness. In contrast with the evaluation of $(R_o/R_2)_{crit.}$, in the computation of $(R_o/R_2)_{cbe}$ the values h_2/R_2 and H_2/R_2 can no longer be considered as zero. If R_o/R_2 is so chosen

TABLE 1

Different Possible Relations
Between the Dimensions h_1, H_1 and L

STAGE	$h_1^* = 0$	$h_1^* < H_1^*$	$h_1^* = H_1^*$	$h_1^* > H_1^*$
INITIAL	$L = 0$	$L = 0$	$L = 0$	$L = 0$
INTER-MEDIATE	$L \lesssim h_1$, $L < H_1$ $L \gtrsim h_1$, $L < H_1$	$L \lesssim h_1$, $L < H_1$ $L > h_1$, $L \lesssim H_1$	$L < h_1$, $L < H_1$ $L < h_1$, $L \gtrsim H_1$	$L < h_1$, $L < H_1$ $L < h_1$, $L \gtrsim H_1$
FINAL	$L > h_1$, $L \gtrsim H_1$	$L < h_1$, $L > H_1$ $L > h_1$, $L > H_1$	$L \gtrsim h_1$, $L > H_1$	$L \gtrsim h_1$, $L > H_1$

*Initial Dimensions

that $v_b/\dot{U} = 0$ from the beginning of the process, $h_2/R_2 = \Delta T/R_2$ and $H_2/R_2 = T_o/R_2 = (T/R_2 + \Delta T/R_2)$, where $\Delta T/R_2$ represents the displacement of the ram between the initial position (T_o/R_2) and any stage (T/R_2) during the process.

As soon as some $(R_o/R_2)_{crit.}$ values were obtained for a specific configuration and different friction values, several curves of the relative pressure as a function of T/R_2 were plotted. The results are given in Fig. 8. As it was mentioned before, the total pressure is the sum of the components: internal power WI, shear losses WS, and friction losses WF. Fig. 9 shows these components and the total relative pressure versus T/R_2 for a friction factor m = 0.25.

A tapered punch is shown in Fig. 10. When tapered surfaces are involved Eq. (1) no longer applies. In such cases, the solution can be obtained by using the UBET computer program (Ref. 4).

When rectangular dies were studied, the solutions by Refs. 2 and 4 were identical. The comparison produced was used for proofing and debugging of both solutions.

Figure 11 illustrates the use of the UBET program for tapered geometries. The figure shows how the relative pressure is affected by changing the ram shape in the combined forward-backward process shown in Fig. 10. Furthermore, Fig. 11 suggests the possibility of optimizing the geometry to get a minimum extrusion force. The same figure shows the effect of a variable geometry on the $v_b/\dot{U}$ and $v_f/\dot{U}$ speeds.

Once the data, as shown in Table 2, are given to the UBET program, the computer divides the figure into elemental triangular and rectangular regions. The extrusion force, together with the final velocity field describing the metal flow through the regions, is obtained by optimizing with respect the pseudoindependent velocities at the so-called arbitrary boundaries. Typical results are shown in Fig. 12 and Tables 3 and 4. Fig. 12 shows the geometry for x = 1 (x is defined in Fig. 10) divided into regions and Table 4 shows the corresponding final velocity field. As it is observed, for this particular case of x = 1, $v_b/\dot{U}$ = 0.72 and $v_f/\dot{U}$ = -2.11. In the UBET program forward velocities are considered positive and vice versa, which is opposite to the sign convention of Ref. 2.

As was mentioned before, an interactive computer program based on the analytical solution (Ref. 2) was created for this study. The program, which can handle the full range of process parameters, is divided into two parts. The first part deals with the combined forward-backward extrusion. For a given geometry it computes the relative pressure entering the backward velocity $v_b/\dot{U}$, or computes the actual p_R/σ_o by optimizing Eq. (1) with respect to the pseudoindependent parameter $v_b/\dot{U}$. The tube-extrusion process is considered in the second part. The program computes the critical upper gap for flash formation and for backward extrusion and simulates one extrusion from initial to final geometry by computing the relative pressure as a function of the thickness of the slug.

TABLE 2

Coordinates of Fig. 7

POINT #	RADIAL	HEIGHT
1	0.25	(5.5-X)
2	1.30	5.5
3	1.30	6.0
4	F1.50	6.0
5	1.50	(5.5-X)/2
6	1.50	0.5
7	0.80	0.5
8	0.80	0.0
9	F0.25	0.0

TABLE 3

UBET Results for a Variable Geometry, m = 0.05

X	Points	Regions	Arbitrary Boundaries	Force	$v_b/\dot{U}$	$v_f/\dot{U}$
0	9	8	3	27.64	-0.79	-3.59
0.5	9	13	6	24.27	-0.30	-3.11
1.0	9	13	6	21.15	0.96	-1.87
1.5	9	13	6	17.47	1.64	-1.22
1.7	9	13	6	16.31	1.85	-1.01
2.0*	8	10	4	15.78	2.21	-0.67
2.5	9	13	6	16.25	2.11	-0.77
3.0	9	13	6	16.93	2.08	-0.79
3.5	9	13	6	16.92	2.01	-0.86
4.0*	8	10	4	16.98	1.85	-1.02
4.5	8	10	4	17.21	2.03	-0.84

*These values were computed after deleting nodal point 5 in Fig. 10.

TABLE 4

Velocity field, X = 1 and m = 0.05

Region	VSUBT	VSUBL	VSUBB	VSUBR
1	-1.00	0	-0.8538	0.1008
2	-0.8538	0	-0.7618	0.0147
3	-0.7618	0	-2.1142	-0.2789
4	-2.1142	0	-2.1142*	0
5	-1.00	0	-0.4292	0.4841
6	-0.4292	0.1008	-0.4523	4.4204
7	-0.4523	0.0147	-0.4851	0.0032
8	-0.4851	-0.2789	0	-0.0597
9	0.7260**	0	0.7260	0
10	0.7260	0.4841	-0.3442	0
11	-0.3442	0.0442	-0.4517	0
12	-0.4517	0.0032	-0.4851	0
13	-0.4851	-0.0597	0	0

where the letters following VSUB stand for top, left, bottom, and right surfaces respectively.

*$v_b/\dot{U}$ = -2.1142
** $v_b/\dot{U}$ = 0.7260

DISCUSSION

The general optimization procedure of the pseudoindependent parameter $v_b/\dot{U}$ is presented in Fig. 3. For the geometry described, the minimum or actual solution is $P_R/\sigma_o = 2.29$ and corresponds to $v_b/\dot{U} = -0.6$. The metal will flow upward at this velocity because this value will minimize the extrusion pressure for the geometry and friction given. Any other ratio of $v_b/\dot{U}$ (and $v_f/\dot{U}$) will require higher pressure. As mentioned before, a negative $v_b/\dot{U}$ value means that some or all of the material is moving upward. For a given process, the principle of volume constancy imposes a negative limit upon $v_b/\dot{U}$. The negative limit is given by

$$v_b/\dot{U}\Big|_{max} = [1 - (R_i/R_o)^2]/[1 - (R_o/R_2)^2] \qquad (5)$$

and represents the case in which all the material is moving backward due to the fact that $R_i/R_2 \approx R_1/R_2$. This value is indicated in the figure as $v_b/\dot{U}\Big|_{max} = -1.6178$.

For the process analyzed in Fig. 3, $v_b/\dot{U} < v_b/\dot{U}\Big|_{max}$ and therefore it corresponds to a case of combined forward-backward extrusion. In other words, not all the material is moving up.

On the positive side, the maximum speed that can be obtained is $v_b/\dot{U} = 1$ and this is associated with a forward extrusion that can be produced with a very small upper gap.

In Fig. 4 the results clearly show the variation of $v_f/\dot{U}$ and $v_b/\dot{U}$ as a function of the upper gap when the rest of the process parameters remain constant. According to the volume constancy principle, $v_f/\dot{U}$ and $v_b/\dot{U}$ are related through Eq. 3. The former equation can be rewritten in this case as

$$v_f/\dot{U} = A - \frac{v_b/\dot{U}}{B} \left[1 - (R_o/R_2)^2\right] \tag{6}$$

where A and B are constants given by $A = [1 - (R_i/R_2)^2]/B$ and $B = (R_1/R_2)^2 - (R_i/R_2)^2$. If the relative $v_b/\dot{U}$ is constant, the Eq. (6) can be expressed in the following way

$$v_f/\dot{U} = D + C(R_o/R_2)^2 \tag{7}$$

where C and D are constants given by $C = [v_b/\dot{U}]/B$ and $D = A - C$

In the same manner it can be demonstrated that when $v_f/\dot{U}$ is a constant value the relative velocity $v_b/\dot{U}$ should change according to

$$v_b/\dot{U} = E/[(R_o/R_2)^2 - 1] \tag{8}$$

where $E = \text{Constant} = (v_f/\dot{U}) [(R_1/R_2)^2 - (R_i/R_2)^2] + (R_i/R_2)^2 - 1$

When the relative velocity $v_b/\dot{U}$ is equal to one (for small values of R_o/R_2), $v_f/\dot{U}$ increases continuously according to Eq. (7). Physically, it means that for small gaps between the ram and the chamber, the material at the upper gap moves downward with the ram,

causing the velocity $v_f/\dot{U}$ to increase due to an increase in the amount of metal extruded forward. As it is observed from Fig. 4, this situation can exist up to a certain critical gap or R_o/R_2 value called $(R_o/R_2)_{crit.}$. If this specific gap is increased by a very small amount, the velocity $v_b/\dot{U}$ will drop to zero and the material at the upper gap will be stationary while the ram keeps going down so that a flash starts to form. For $v_b/\dot{U} = 0$, Eq. (6) indicates that $v_f/\dot{U}$ should be constant. All this is in agreement with Fig. 4, in which $v_f/\dot{U}$ remains constant for the whole range of $v_b/\dot{U} = 0$. This region of $v_b/\dot{U} = 0$ is associated with a flash formation and is defined by the values $(R_o/R_2)_{crit.}$ and $(R_o/R_2)_{cbe}$ as is shown in Fig. 4.

When the gap is increased even more, the material at the upper gap will start moving up, which, according to the sign convention (Ref. 2), means a negative $v_b/\dot{U}$ value. This velocity increases up to a certain value until the forward metal flow becomes constant again. Eq. (8) shows that if $v_f/\dot{U}$ remains constant the velocity $v_b/\dot{U}$ should decrease as R_o/R_2 rises. This effect is observed in Fig.4 when $v_f/\dot{U}$ is at constant values of 2.08 and 1.00.

The curves in Fig. 4 clearly identified the general trend of the forward and backward flow when the upper outer radius R_o/R_2 is increased. For $R_o/R_2 < (R_o/R_2)_{crit}$ values, all the material moves forward and the process corresponds to a tubular forward extrusion. For $(R_o/R_2)_{crit} < R_o/R_2 < (R_o/R_2)_{cbe}$ a flash will result but backward extrusion will not prevail. With larger gap the process changes

into a combined forward-backward extrusion with a backward flow of increasing and decreasing velocity which finally approaches the value corresponding to $v_f = 0$ and given by

$$v_b/\dot{U} = [(R_i/R_2)^2 - 1]/[(R_o/R_2)^2 - 1] \qquad (9)$$

In reality, $v_f/\dot{U}$ is greater than zero and therefore $v_b/\dot{U}$ is smaller than given by Eq. (9).

It should be noticed, however, that the curves were obtained for a specific slug thickness T/R_2 and therefore only represent an instantaneous position during the actual extrusion process. Consequently, the $(R_o/R_2)_{crit}$ value and the range for $v_b/\dot{U} = 0$ should change as the extrusion proceeds.

The curves shown in Fig. 6 indicate that the critical gap $(R_o/R_2)_{crit}$, independently of the friction level, always decreases as the extrusion proceeds. However, all the curves approach $(R_o/R_2)_{crit.}=1$ as T/R_2 approaches zero and the change of $(R_o/R_2)_{crit.}$ is larger for low friction values. Obviously, a low friction not only gives lower extrusion pressures but also allows for a larger critical gap and therefore reduces the possibility of flash formation during the forward extrusion.

In the same way that $(R_o/R_2)_{crit.}$ changes as T/R_2 decreases, some variation of the range for $v_b/\dot{U} = 0$ (Fig. 4), given by $[(R_o/R_2)_{crit.} - (R_o/R_2)_{cbe}]$, should be expected if this range could

be represented graphically in Fig. 7.

However, the evaluation of $(R_o/R_2)_{cbe}$ for any process that starts below the $(R_o/R_2)_{crit.}$ curve is complex. The friction between the forming flash and the surface of the ram associated with h_2/R_2 will affect the formation of the flash, making it difficult to obtain the actual h_2/R_2 and H_2/R_2 dimensions used in the computation of $(R_o/R_2)_{cbe}$. On the other hand, if R_o/R_2 is over the $(R_o/R_2)_{crit.}$ at the beginning of the process, h_2/R_2 will be equal to $\Delta T/R_2$ and H_2/R_2 to $(\Delta T/R_2 + T/R_2)$ during the entire process, making it possible to obtain the curve of $(R_o/R_2)_{cbe}$ as is shown in Fig. 7.

The same criterion presented in Table 1 was applied in choosing the values h_1/R_2 and H_1/R_2 to obtain $(R_o/R_2)_{cbe}$. However, the L/R_2 value was given by

$$L/R_2 = \Delta T/R_2 \, [2 - (R_i/R_2)^2 - (R_o/R_2)^2]/[(R_1/R_2)^2 - (R_i/R_2)^2] \quad (10)$$

This equation was derived by assuming $v_b/\dot{U} = 0$ from the beginning of the extrusion and therefore R_o/R_2 should be greater than $(R_o/R_2)_{crit.}$ for T_o/R_2.

As examples, two processes are illustrated in Fig. 7, one with $R_o/R_2 = 1.015$ and the other with $R_o/R_2 = 1.06$. The first one represents a tubular extrusion that occurs without flash until T/R_2=0.39. The other process describes a tube extrusion with flash until the slug becomes equal to $T/R_2 = 0.18$. Any further extrusion after this point,

or R_o/R_2 values above the $(R_o/R_2)_{cbe}$ curve, will produce a combined forward-backward extrusion.

Fig. 7 can also give an idea of what minimum upper thickness can be obtained in the case of a combined forward-backward extrusion. For the parameters used in Fig. 7 the minimum relative wall thickness is equal to 1.085.

Curves of the relative ram pressure versus the slug length in Fig. 8 show how p_R/σ_o behaves as the tube extrusion proceeds. For friction values different from zero, the curves present an initial peak which becomes more pronounced as the friction increases. This initial increase of p_R/σ_o is originated by the new friction losses between the emerging extrudate, the mandrel, and the H_1/R_2 portion of the die. The stroke length difference $\Delta T/R_2$, between the initiation of the extrusion and the thickness at which the peak occurs, represents the distance travelled by the ram until the complete mandrel is covered by the extrudate tube ($h_1 = L$) and the emerging part has gone over the H_1/R_2 distance ($H_1 = L$). As it is observed from Fig. 8, the length $\Delta T/R_2$ is independent of the friction level and therefore depends only on the geometry of the process.

Figure 9 presents the different components of the total relative pressure as functions of T/R_2. The shear losses component always decreases with T/R_2 in the early stages of the extrusion. However, at the beginning, the reduction in the shear losses is overpassed by the increasing new friction losses of the tubular extrudate. Once

the tube becomes larger than the h_1/R_2 mandrel portion and the H_1/R_2 dimension, the shear losses become predominant and the total relative pressure begins to decrease again. Obviously, the minimum represents a balance between the shear losses and the friction losses.

At the end of the stroke, as the slug becomes smaller, the total relative pressure rises again. Friction losses along ram and bottom die surfaces due to a radial flow of metal are the cause for the final increase of p_R/σ_o. This can be deduced by observing how the friction component in Fig. 9 rises quickly at the end of the stroke or by noticing that the minimum of the curves in Fig. 8 occurs earlier as the friction increases.

It is interesting to observe that the internal deformation component remains constant during the process and that, in contrast to the direct extrusion process, the friction losses always increase as the extrusion proceeds.

It is important to remember that in practice there should be another peak in the ram pressure curve before the peak due to the friction on the mandrel and outer lower die is reached. As it is known, this initial peak occurs when the dead zone shears off the billet (after the elastic adjustment of the slug and the equipment) and pressure drops due to a new lower friction between billet and dead zone. However, the solution of Ref. 2 does not account for dead-zone formation. The dead zone is handled properly when the UBET computer program is used.

The results in Fig. 11 illustrate that the UBET program can solve extrusion processes of a large variety of geometries in a fairly simple way and without going into a consuming time analysis for each shape to obtain such an upper-bound solution as the one given by Eq. (1). A more complex shape with tapered ram is shown in Fig. 10. Rather than repeating an analysis for each change and chamfer introduced in the die design, the general "UBETS" program will now be employed. In order to solve a problem, the UBET program required only the nodal points of the figure and the friction value. The nodal points are entered as is shown in Table 2 and in clockwise manner as is shown in Fig. 10. Flash openings are indicated by a letter F written before the second coordinate which defines a gap (see Table 2).

In this case, the height of nodal point 1 was taken as the variable increasing the x value. The extrusion force obtained for each x value is plotted in Fig. 11. Substantial variations of the force are observed in this figure. The required extrusion force decreases down to a minimum. Larger x values will increase the force due to the fact that a larger x means a larger ram area and, as a result, the increasing friction losses become the dominating factor of the total force. "UBETS" was used to demonstrate its usefulness in finding the optimal taper to minimize extrusion force.

Some scattering of the resulting points may be expected and can be minimized if enough computing time is spent on the optimizer of "UBETS". The more broadly the optimizer operates, the smaller is the

scatter. Each point in Fig. 11 represents the minimum obtained of at least five evaluations of the same configuration.

Once again, it should be remembered that the results of Fig. 11 correspond to an instantaneous ram position. So, as the extrusion proceeds, the value x that optimizes the force will change. In that case it would be useful to plot on the same figure curves like the one in Fig. 8 showing the extrusion force for different stages of the process but with x as a parameter. Since x has to be constant during the actual extrusion, an overall evaluation would have to be done, in order to obtain an optimal configuration, in such a way that the x value corresponds to an optimum process and not only to an optimum result of an instantaneous stage of the extrusion.

Such evaluation could be done using as a criterion the minimum force (capacity of the press) or the minimum area under the plot of force vs. stroke displacement (energy associates with the process).

As it is observed in Fig. 11, the changes in the taper of the punch are reflected not only in the total required pressure but also in the relative speeds $v_f/\dot{U}$ and $v_b/\dot{U}$.

CONCLUSIONS

A numerical analysis of the combined forward-backward extrusion and the tubular extrusion processes was performed to show the effects of different geometries on the extrusion pressure and the metal flow characterized by the forward and backward velocities.

The present work provides a means for evaluating the effects of the upper gap dimensions in combined forward-backward extrusion. The numerical results have demonstrated the existence of the critical gaps $(R_o/R_2)_{crit.}$ and $(R_o/R_2)_{cbe}$ for forward extrusion without flash, forward extrusion with flash and combined forward-backward extrusion. It was found that for a given slug thickness, the lower the friction was, the higher the $(R_o/R_2)_{crit.}$ value. The $(R_o/R_2)_{cbe}$ criterion can be applied successfully provided that the R_o/R_2 relative radius of the process is always above the $(R_o/R_2)_{crit.}$ curve for any value of T/R_2.

A simulation computer program for tube extrusion was made on the basis of the mathematical expression for combined forward-backward extrusion (Ref. 2). The computer program can be used to evaluate $(R_o/R_2)_{crit.}$, $(R_./R_2)_{cbe}$, and the changes in the extrusion pressure p_R/σ_o during a tube extrusion. The simulation of the tubular extrusion has been carried out by considering successive instantaneous stages and taking into account variation in geometry for each stage. The active friction between the extrudate tube, mandrel, and die surfaces was considered in the simulation. Extrusion pressures are

significantly influenced by this active friction, mainly during the early stages of the extrusion.

The numerical study of tapered configurations was done with the UBET computer program (Ref. 4). This program was demonstrated to be a most practical and general means to obtain extrusion pressures and velocity fields for extrusions of axisymmetric geometry. The numerical UBET results showed that by analyzing a tapered configuration it is possible to optimize an extrusion process for a given stage and therefore for a given process with respect to the total energy or the maximum force required by the process.

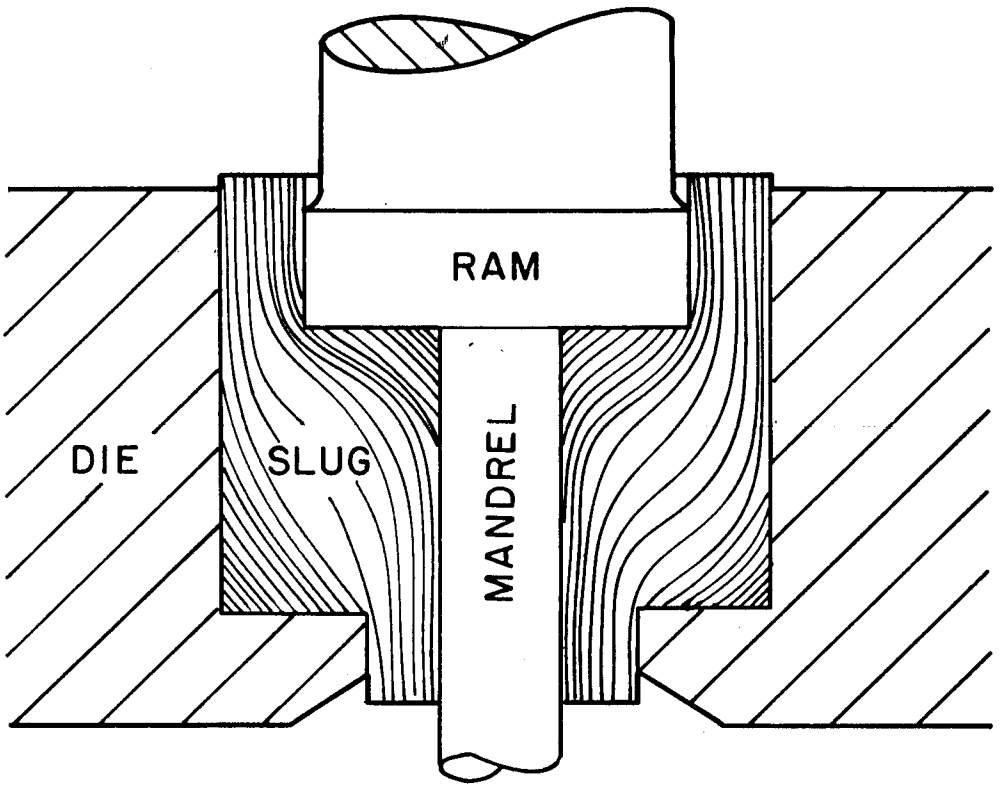

a. FLAT FACES

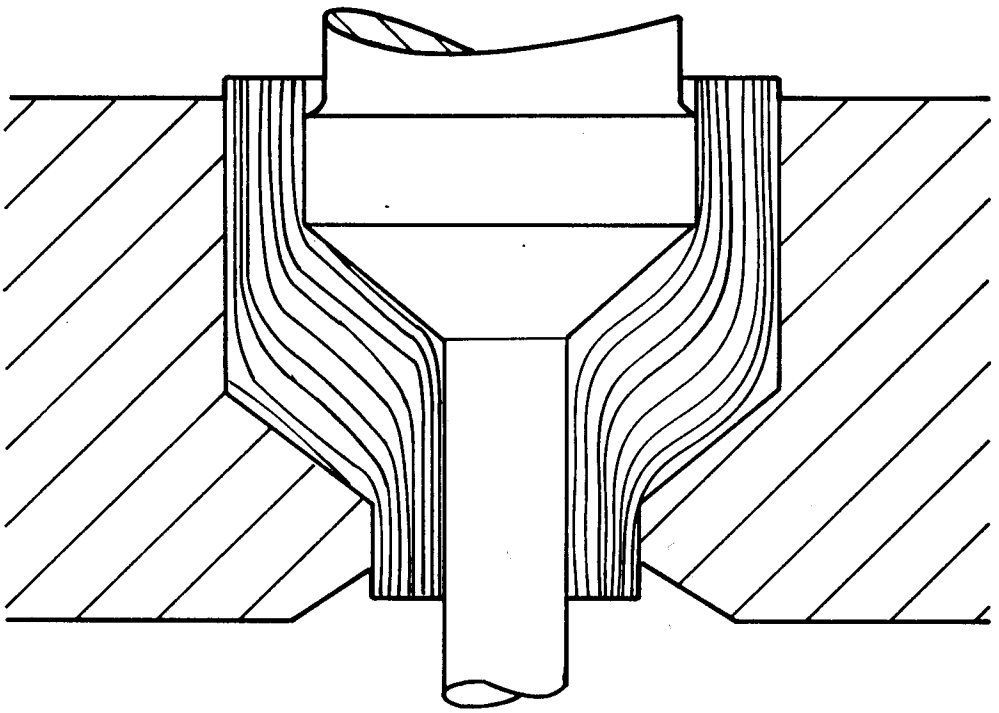

b. TAPERED FACES

FIGURE I THE PROCESS OF COMBINED FORWARD-BACKWARD EXTRUSION WITH DIFFERENT TOOL SHAPES.

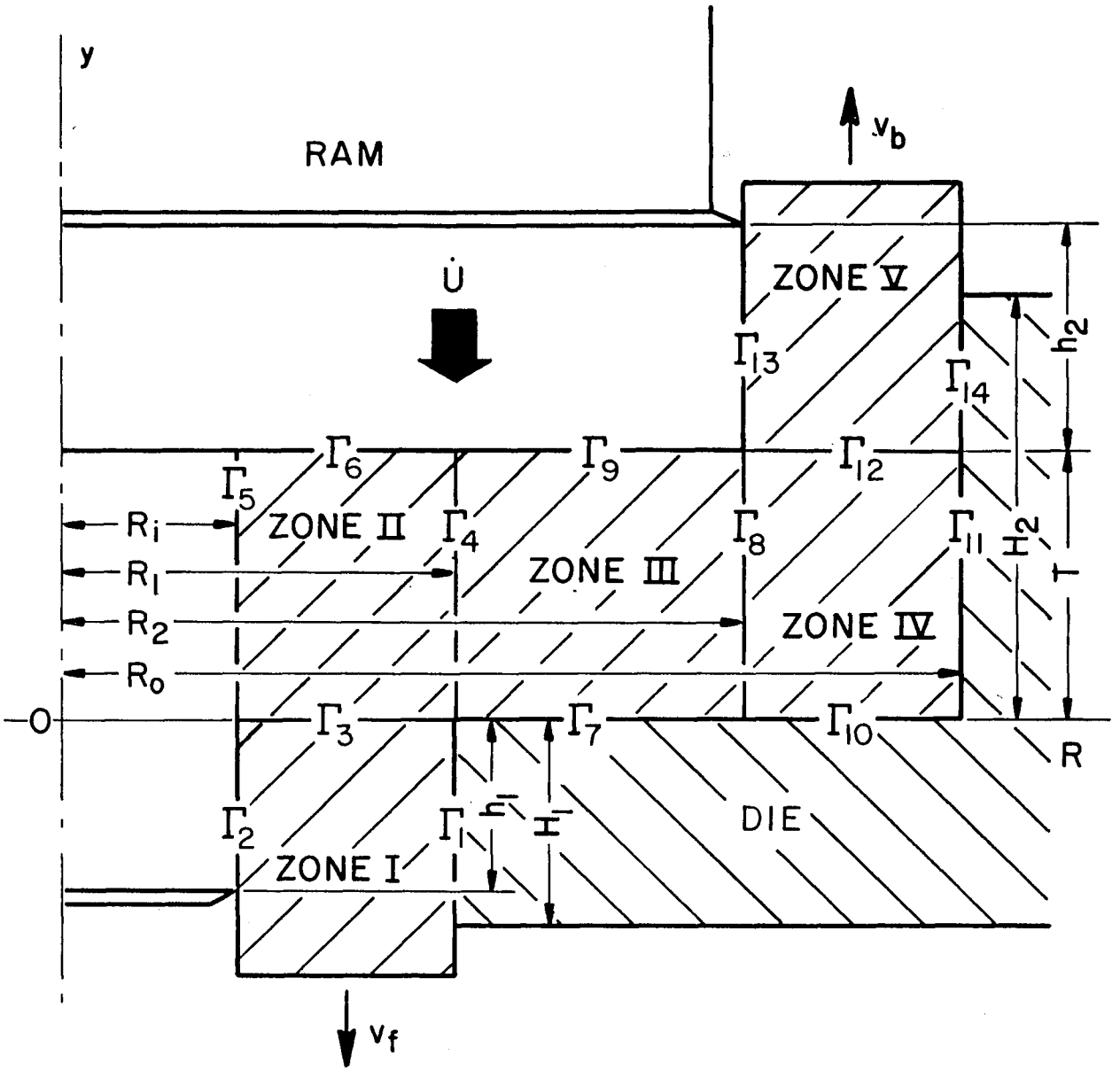

FIGURE 2 GEOMETRY OF COMBINED FORWARD-BACKWARD EXTRUSION.

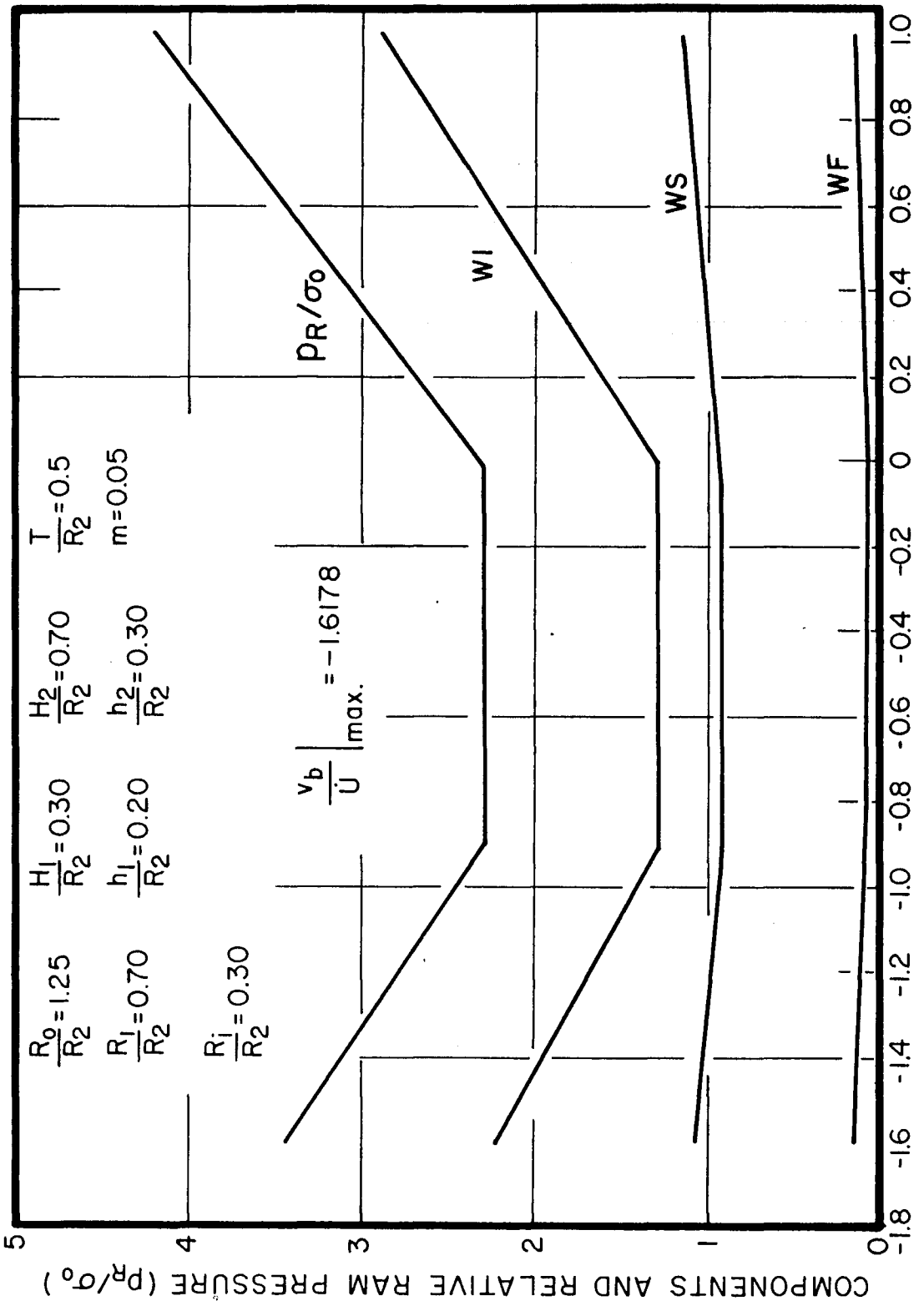

FIGURE 3 OPTIMIZATION OF THE RELATIVE RAM PRESSURE.

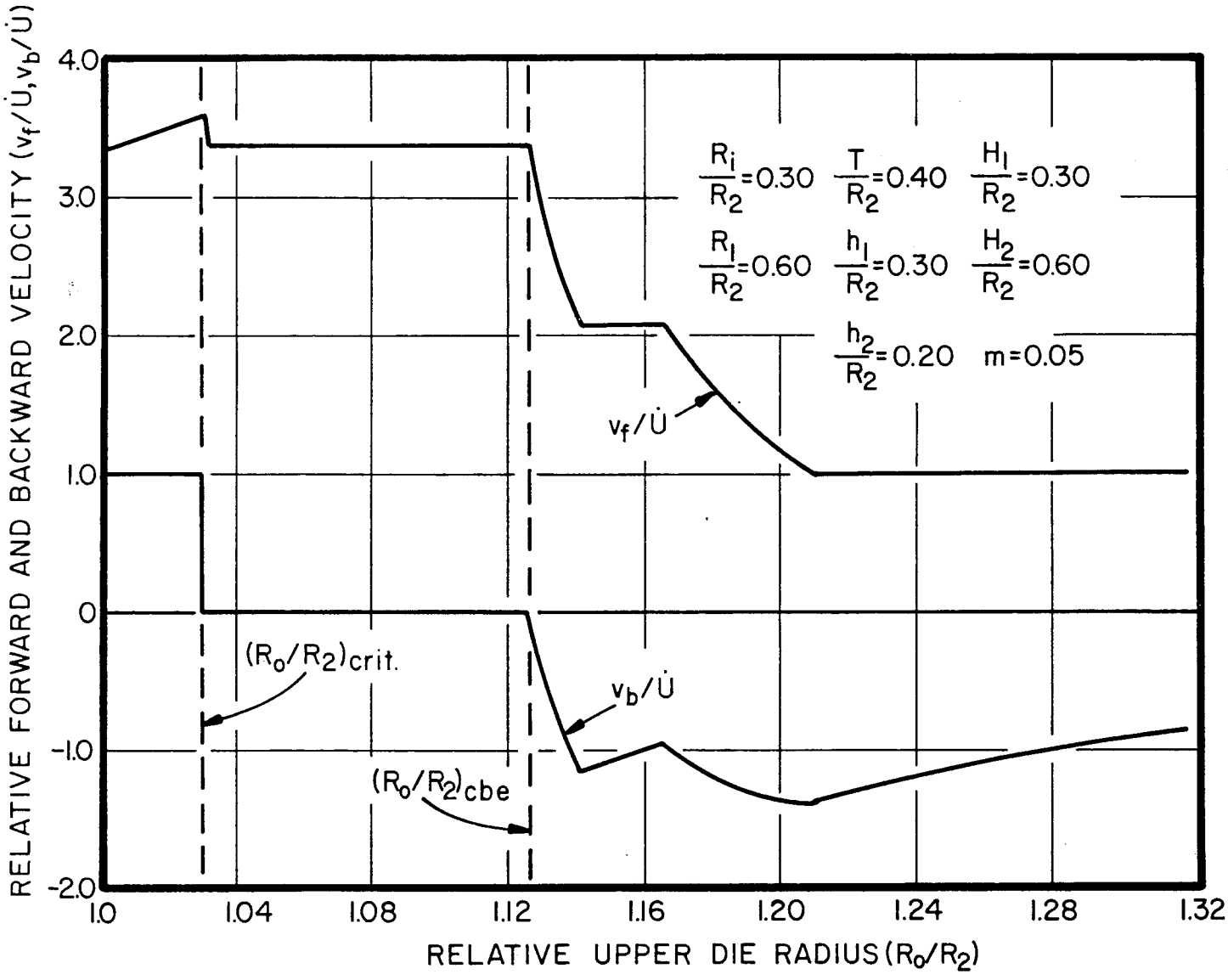

FIGURE 4 VARIATIONS OF $v_f/\dot{U}$ AND $v_b/\dot{U}$ WITH R_o/R_2.

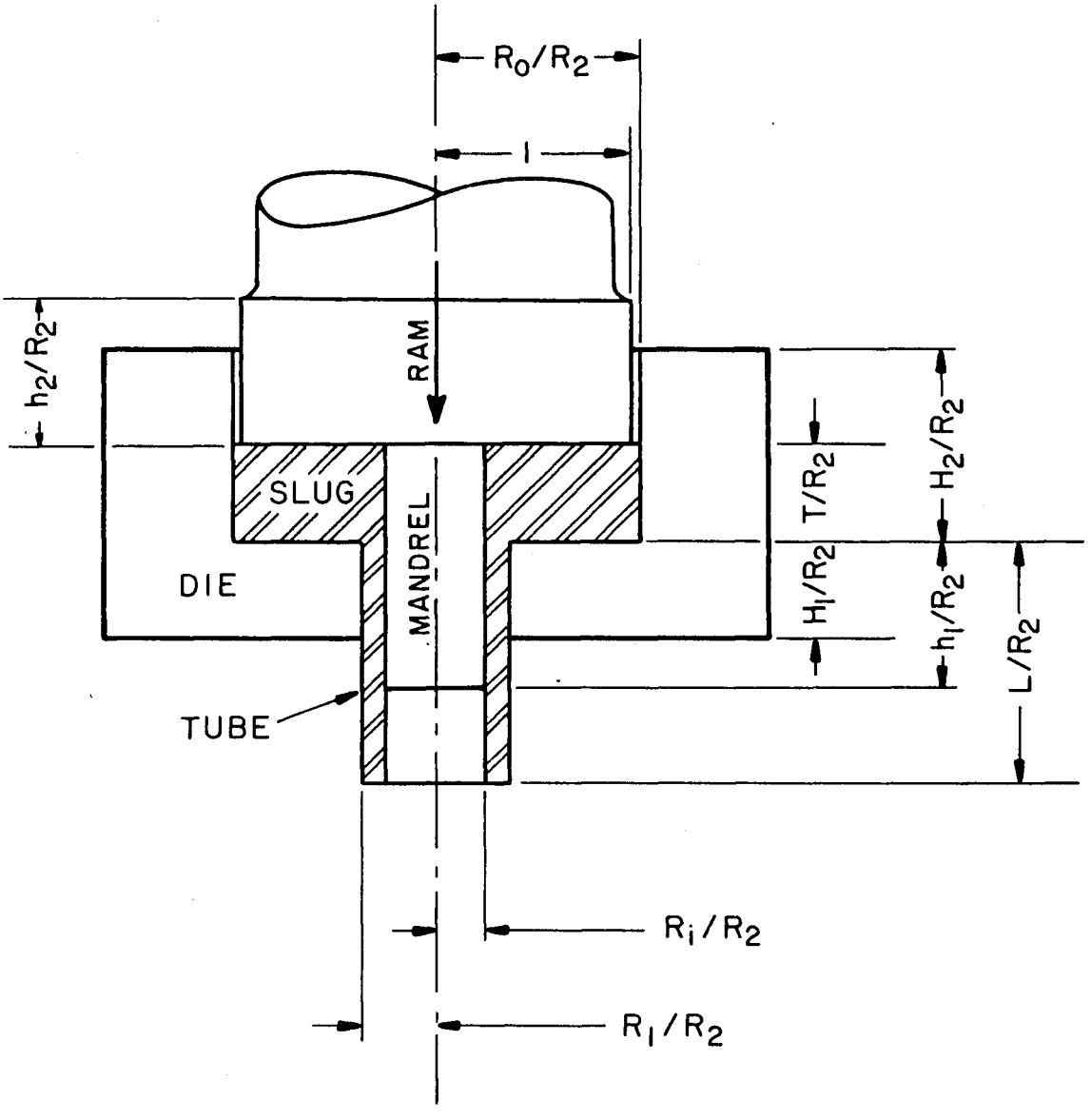

FIGURE 5 FORWARD TUBE EXTRUSION

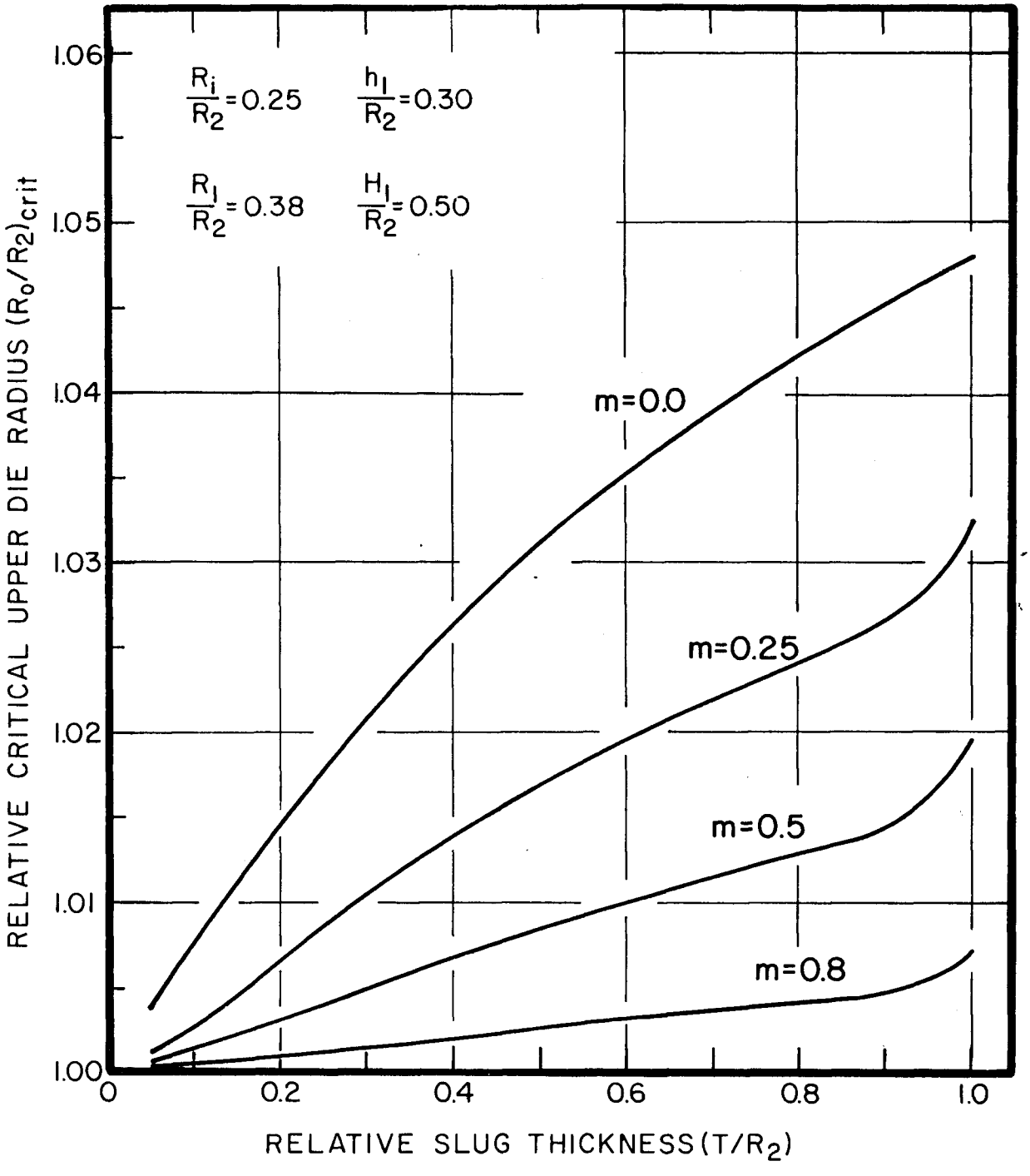

FIGURE 6 VARIATION OF $(R_o/R_2)_{crit.}$ DURING ONE PROCESS.

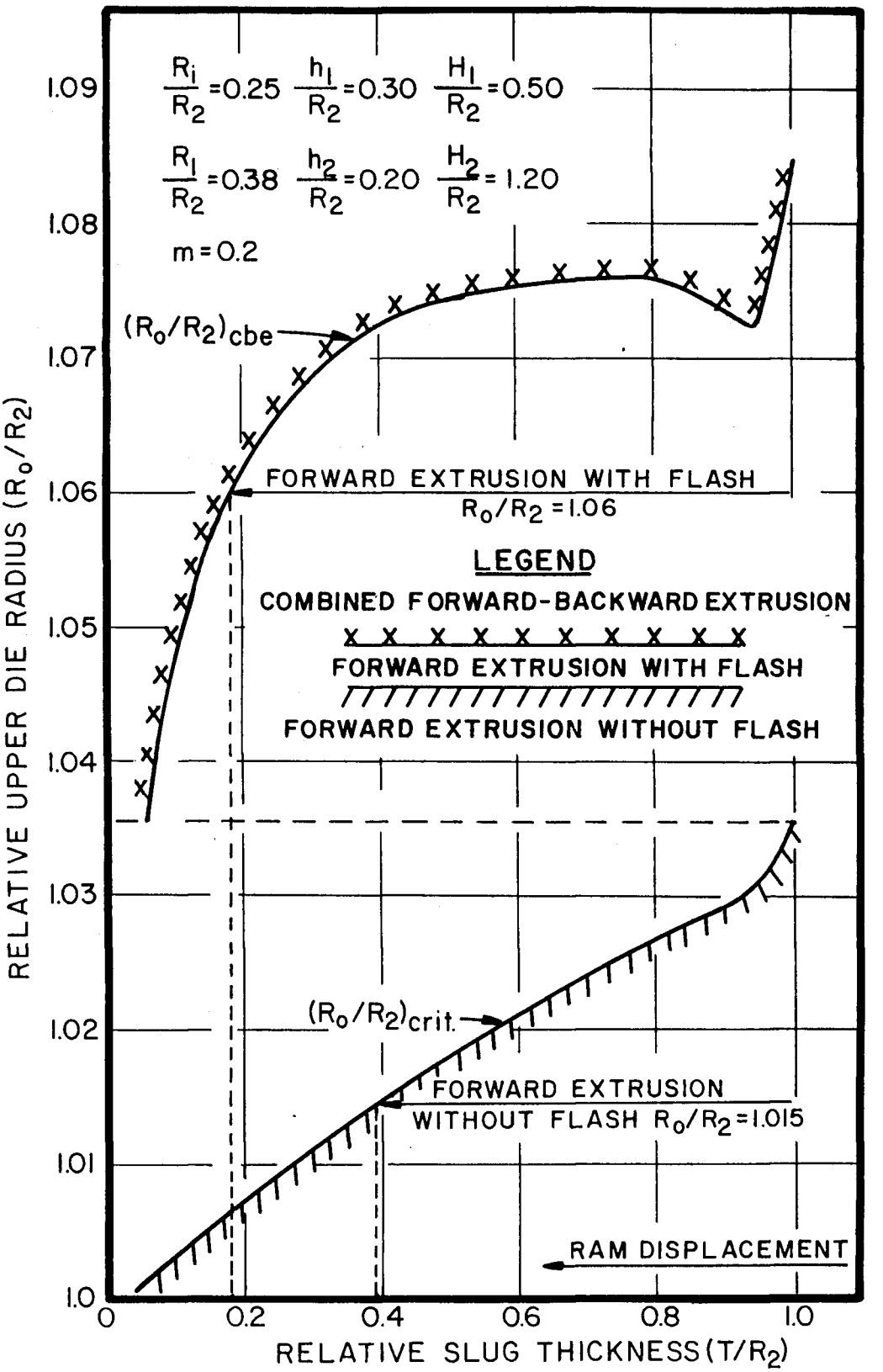

FIGURE 7 CHANGES IN $(R_O/R_2)_{crit.}$ AND $(R_O/R_2)_{cbe}$ DURING ONE PROCESS.

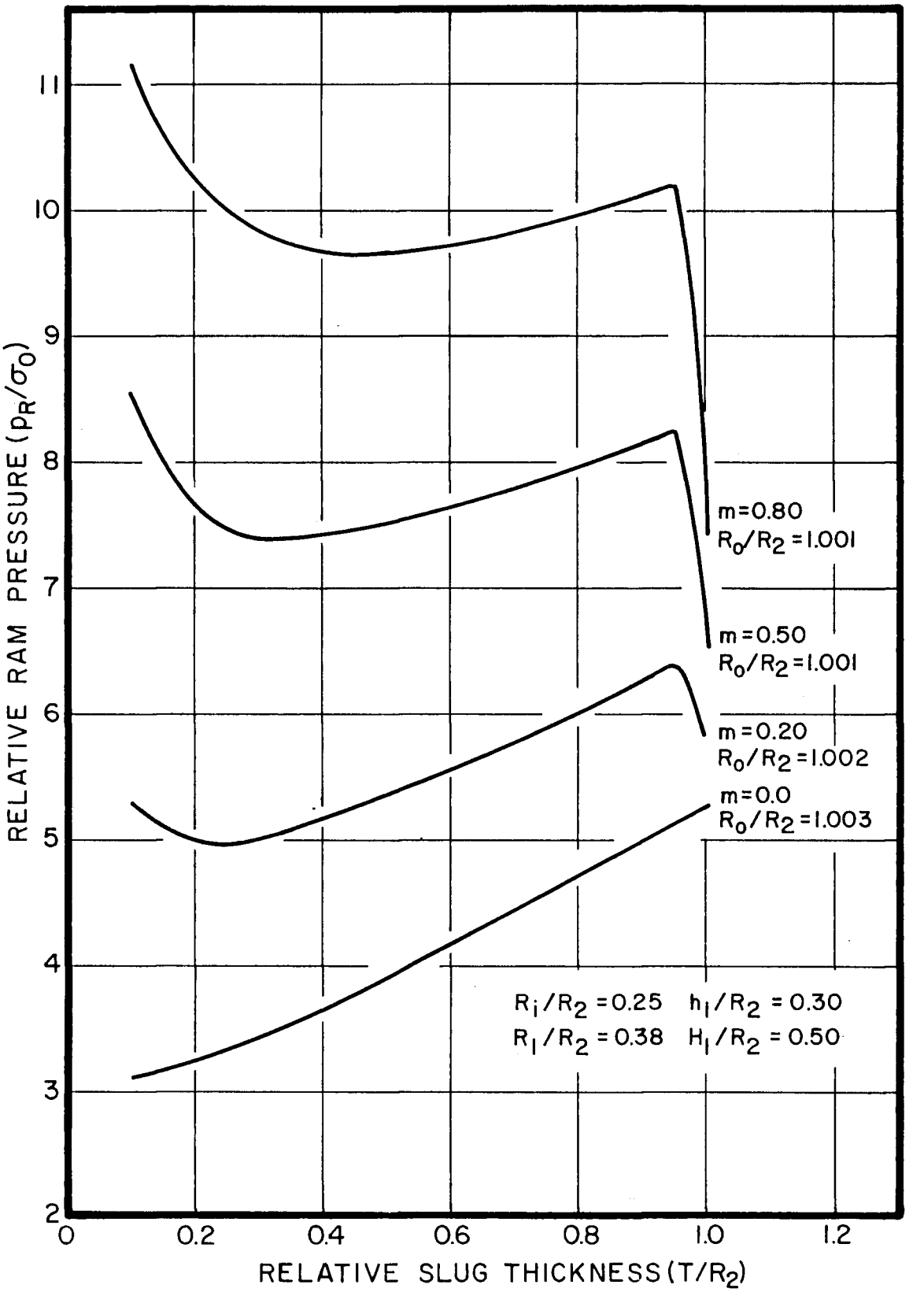

FIGURE 8 VARIATION OF p_R/σ_0 DURING ONE PROCESS.

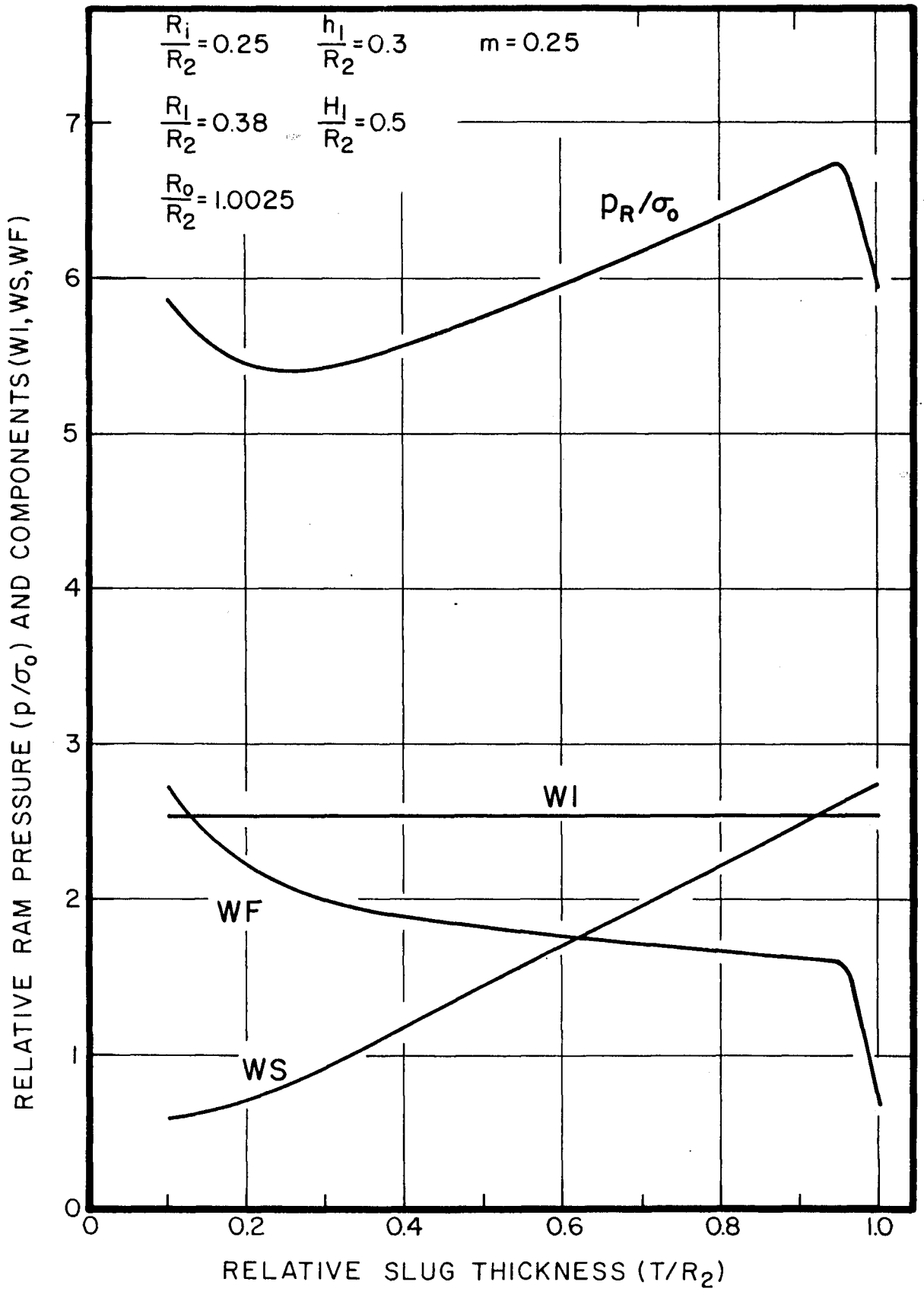

FIGURE 9 VARIATION OF THE RELATIVE PRESSURE COMPONENTS DURING ONE TUBULAR EXTRUSION.

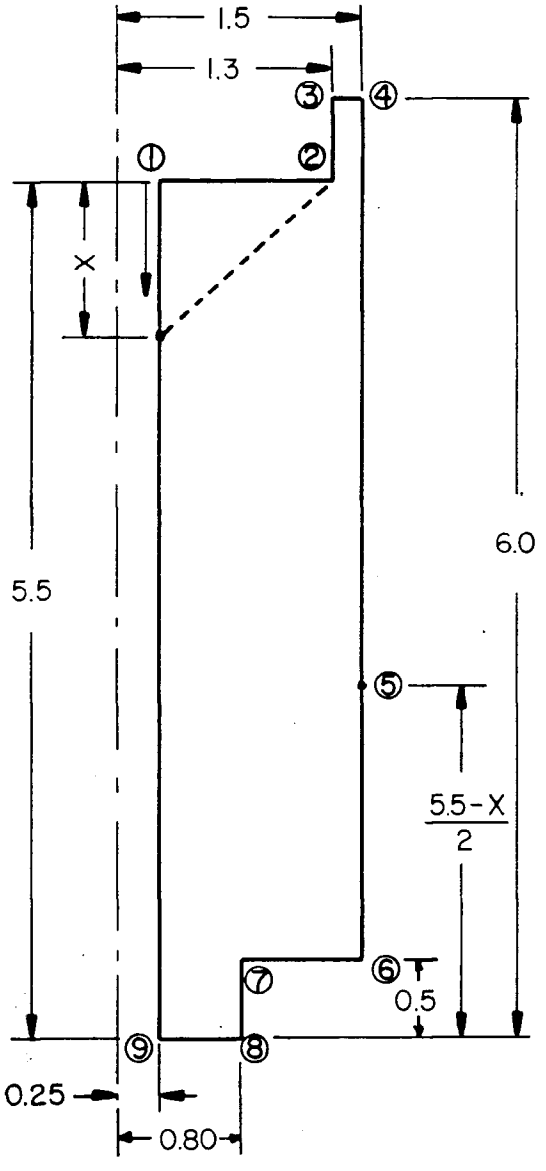

FIGURE 10 FORWARD-BACKWARD EXTRUSION WITH TAPERED GEOMETRY.

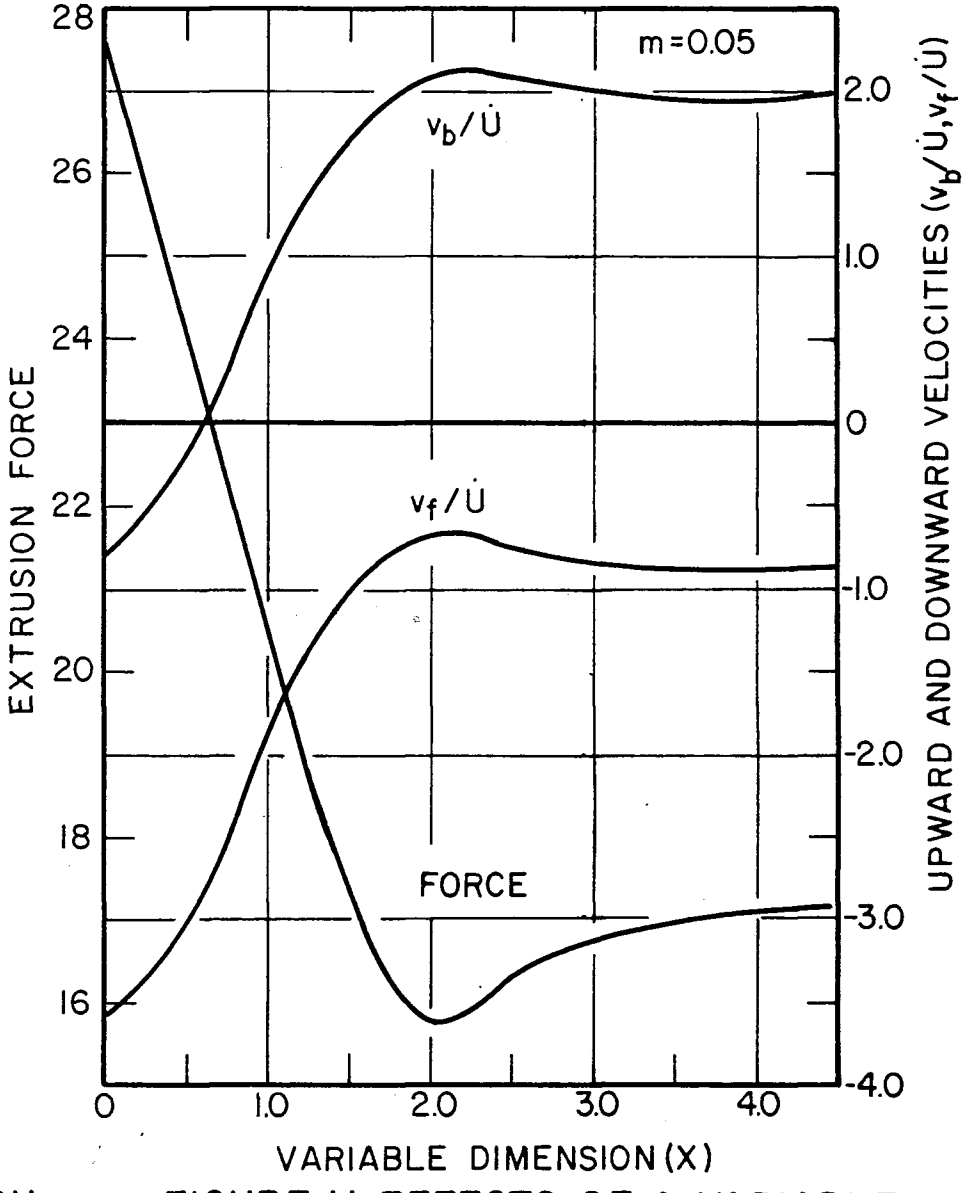

FIGURE 11 EFFECTS OF A VARIABLE GEOMETRY.

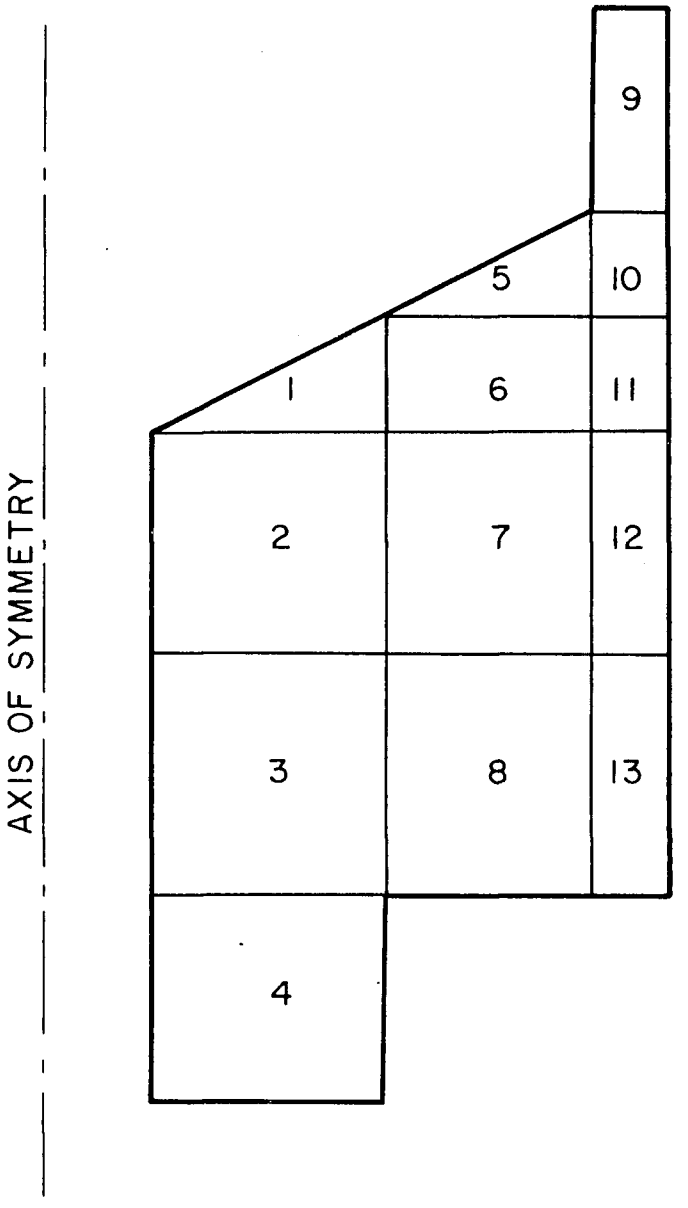

FIGURE 12 GEOMETRY DIVIDED INTO REGIONS BY THE UBET PROGRAM. (CASE OF 9 NODAL POINTS, TABLE 3)

REFERENCES

1. "Metal Progress," Vol. III, No. 2, February 1977, p. 52-57.

2. Avitzur, B., Hahn, W.C., Jr., and Mori, Masahiro, "Analysis of Combined Backward-Forward Extrusion," Journal of Engineering for Industry, Trans. ASME, Vo. 98, No. 2, May 1976, p. 438-445.

3. Avitzur, B., "Metal Forming: Processes and Analysis," McGraw-Hill, New York, N.Y., 1968, 500 pages.

4. Cramphorn, A.S., Bramley, A.N., and McDermott, R.P., "UBET Related Developments in Forging Analysis," Proceedings of the 4th North American Metal Working Research Conference, NAMRC-N, May 17-19, 1976, Columbus, Ohio, p. 80-86.

5. Avitzur, B., "Metal Forming: The Application of Limit Analysis," Annual Review of Material, 1977, 7:261-300, Annual Review Inc.

6. Avitzur, B., "Metal Forming Processes," John Wiley, New York, 1979.

APPENDIX

Simplified flow chart for computer program of combined forward-backward extrusion and tube-forming extrusion based on Eq. (1).

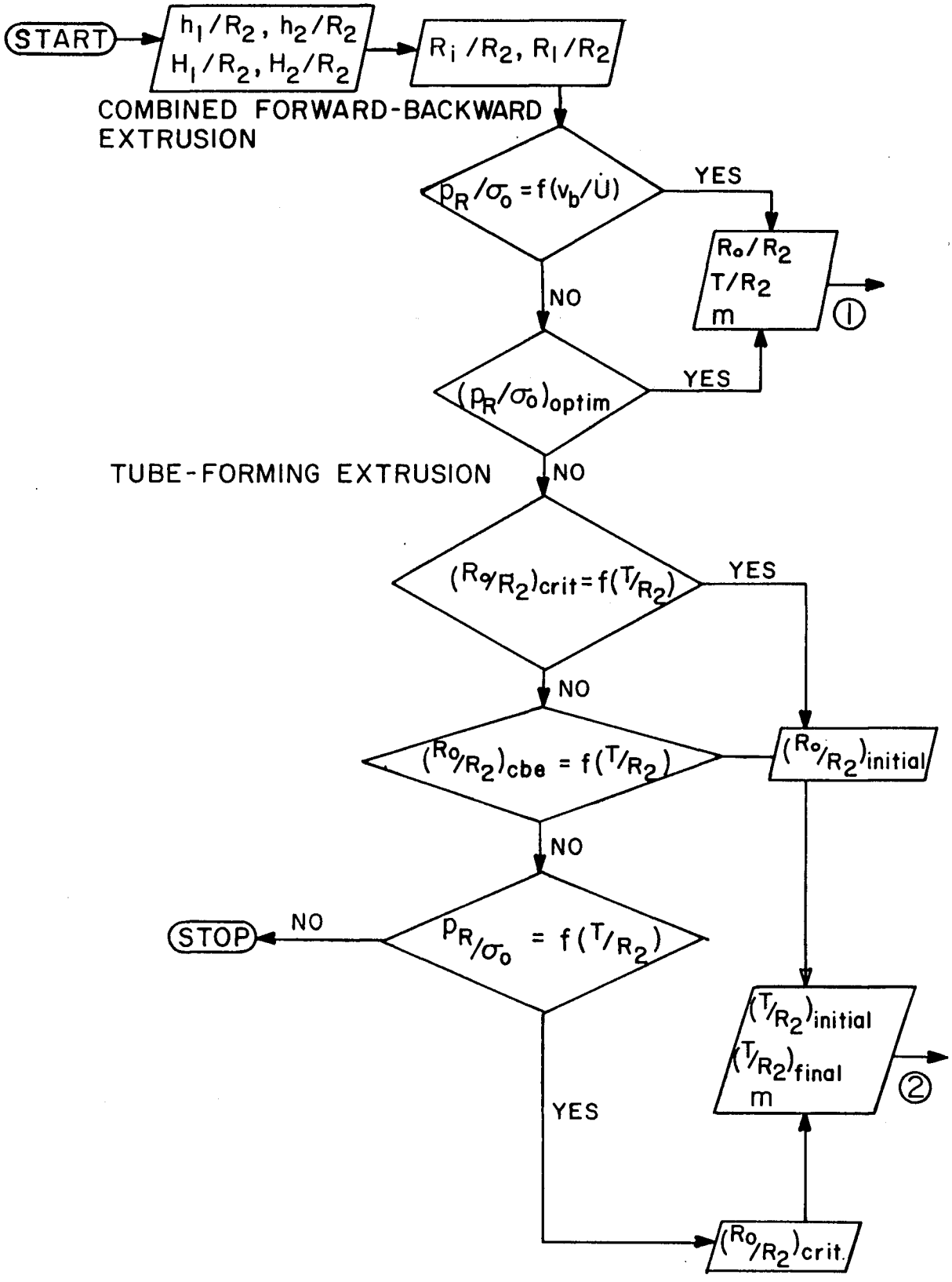
START
h_1/R_2, h_2/R_2
H_1/R_2, H_2/R_2
R_i/R_2, R_1/R_2
COMBINED FORWARD-BACKWARD EXTRUSION
$p_R/\sigma_o = f(v_b/\dot{U})$
YES
R_o/R_2
T/R_2
m
①
NO
$(p_R/\sigma_o)_{optim}$
YES
TUBE-FORMING EXTRUSION
NO
$(R_o/R_2)_{crit} = f(T/R_2)$
YES
NO
$(R_o/R_2)_{cbe} = f(T/R_2)$
$(R_o/R_2)_{initial}$
NO
STOP
NO
$p_R/\sigma_o = f(T/R_2)$
$(T/R_2)_{initial}$
$(T/R_2)_{final}$
m
②
YES
$(R_o/R_2)_{crit.}$

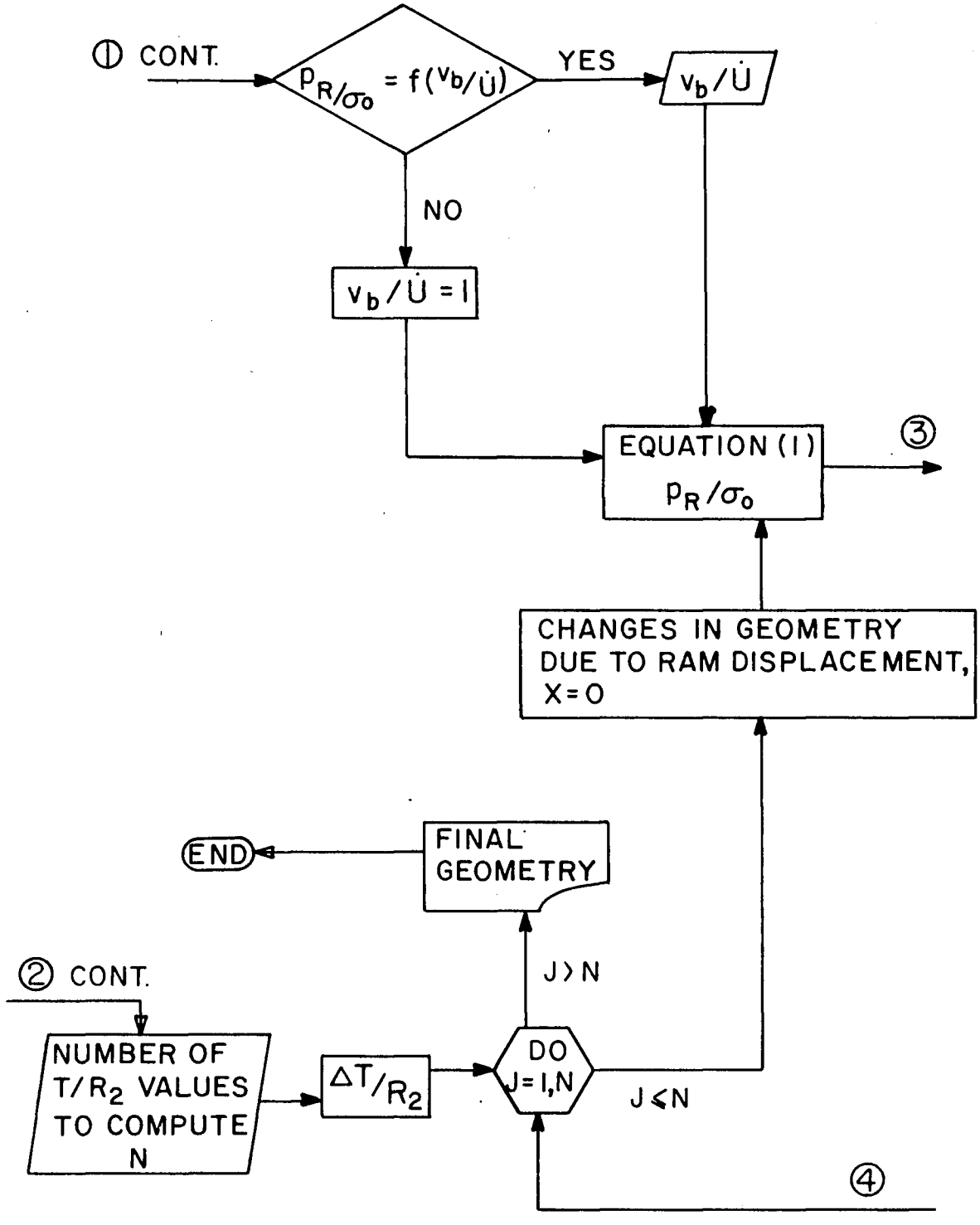
① CONT.
$p_{R/\sigma_o} = f(v_b/\dot{U})$
YES
$v_b/\dot{U}$
NO
$v_b/\dot{U} = 1$
EQUATION (1)
p_R/σ_o
③
CHANGES IN GEOMETRY DUE TO RAM DISPLACEMENT, X=0
END
FINAL GEOMETRY
② CONT.
J > N
NUMBER OF T/R_2 VALUES TO COMPUTE N
$\Delta T/R_2$
DO J=1,N
J ≤ N
④

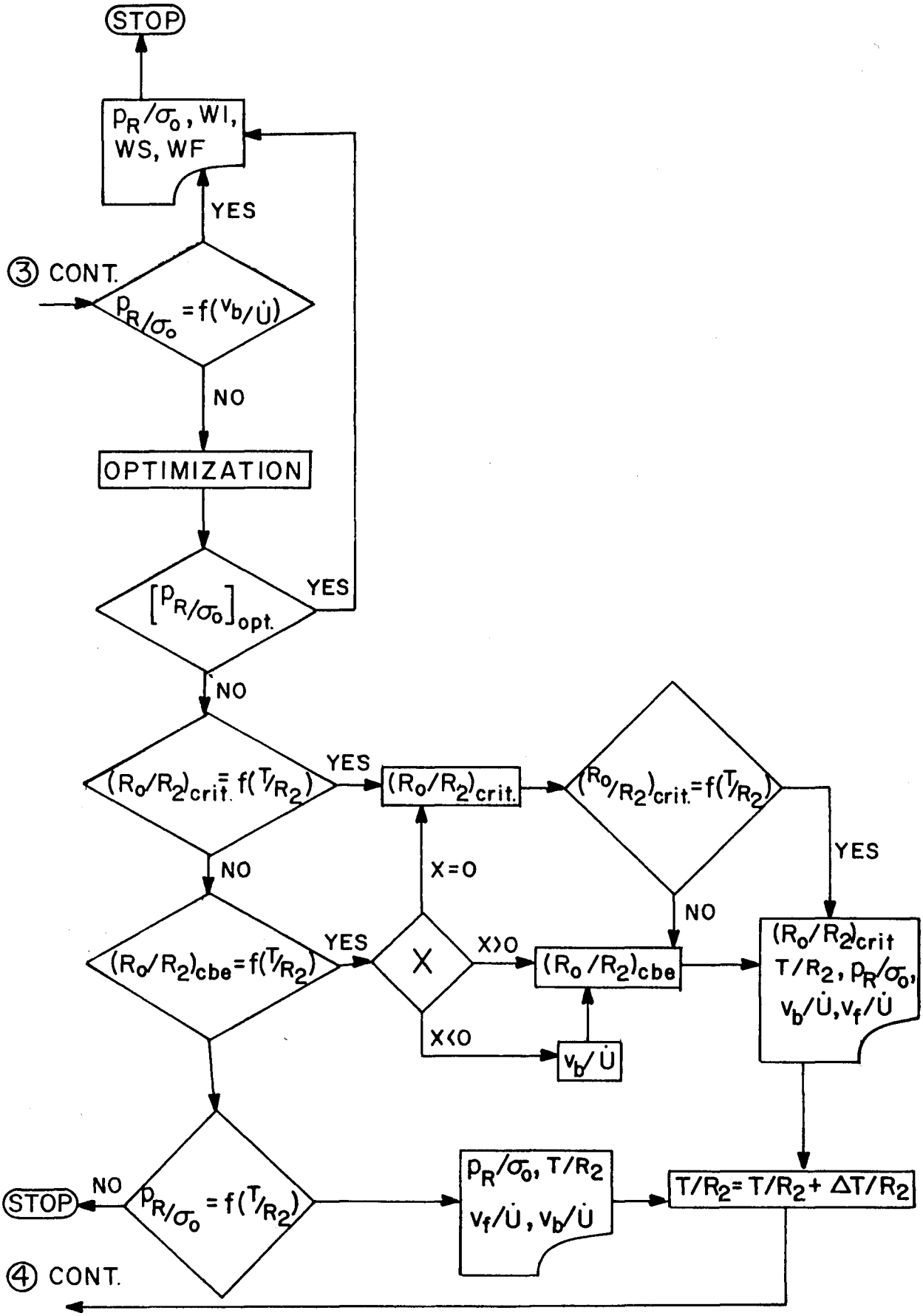
STOP
p_R/σ_o, WI, WS, WF
YES
③ CONT.
$p_R/\sigma_o = f(v_b/\dot{U})$
NO
OPTIMIZATION
$[p_R/\sigma_o]_{opt.}$
YES
NO
$(R_o/R_2)_{crit.} = f(T/R_2)$
YES
$(R_o/R_2)_{crit.}$
$(R_o/R_2)_{crit.} = f(T/R_2)$
YES
NO
X=0
$(R_o/R_2)_{cbe} = f(T/R_2)$
YES
X
X>0
$(R_o/R_2)_{cbe}$
$(R_o/R_2)_{crit}$ T/R_2, p_R/σ_o, $v_b/\dot{U}$, $v_f/\dot{U}$
X<0
$v_b/\dot{U}$
STOP
NO
$p_R/\sigma_o = f(T/R_2)$
p_R/σ_o, T/R_2 $v_f/\dot{U}$, $v_b/\dot{U}$
$T/R_2 = T/R_2 + \Delta T/R_2$
④ CONT.

VITA

Carlos E. Umana was born on November 16, 1947 in San Jose, Costa Rica, to Humberto J. and Miriam Umana. He received his secondary education at Saint Francis College in San Jose and was awarded a Bachelor in Mechanical Engineering degree in July, 1972, from the University of Costa Rica. Before entering Lehigh in September, 1975, he was doing consulting and working as a professor at the University of Costa Rica.